Chem. Res. Chinese Universities, 2019, 35(1), 150—156 doi: 10.1007/s40242-019-8199-1

Comb-shaped 2-Methylimidazolium Poly(arylene ether sulfone) Anion Exchange Membranes with High Alkaline Stability

ZHANG Yurong, GE Xiaoguang, ZHAO Chengji and NA Hui*

Alan G. MacDiarmid Institute, College of Chemistry, Jilin University, Changchun 130012, P. R. China

Abstract A series of comb-shaped poly(arylene ether sulfone)s containing pendant 2-methyl-3-alkylimidazolium group(ImPAES-C*x*, *x*=1, 6, 10) was prepared and characterized as novel anion exchange membranes. These ImPAES-C*x* membranes were obtained by benzylic bromination and imidazolium functionalization. The characteristic nano-phase separation structure was formed in membranes with longer alkyl side chains, as confirmed by small-angle X-ray scattering. The nano-phase separation structures endowed ImPAES-C*x* membranes with improved ionic conductivity, dimensional stability(at least 60% decrease water uptake and swelling ratio at 60 °C) and mechanical properties, together with excellent alkaline stability. Especially, ImPAES-C6 membranes possessed enhanced hydroxide conductivity and chemical stability simultaneously. These results suggest that it is a feasible strategy to introduce appropriate length of alkyl side chains into anion exchange membranes(AEMs) to improve the performance.

Keywords Comb-shaped structure; Imidazolium functionalized poly(arylene ether sulfone); Alkaline stability; Membrane

1 Introduction

The alkaline anion exchange membrane fuel cells(AAEMFCs) have attracted more and more attention than the proton exchange membrane fuel cells(PEMFCs)[1,2], primarily because of the advantages of improved oxygen reduction kinetics at higher pH[1,3], the permission of the use of non-precious metal electro-catalysts(*e.g.*, nickel, cobalt)[4,5], and the low over-potential for fuel oxidation and fuel cross-over[1,6]. As one of the core components of AAEMFCs, the polymeric anion exchange membranes(AEMs) should possess excellent dimensional, mechanical and chemical stability, as well as high ionic conductivity. However, it is still a major challenge to develop an ideal AEM material that meets all the above mentioned requirements.

To date, the quaternary ammonium(QA) functionalized AEMs are most extensively studied for AAEMFC applications[7,8]. A variety of QA-functionalized AEMs based on aromatic hydrocarbon polymers have been studied due to their excellent thermal and mechanical stability. They are typically prepared by chloromethylation of aromatic backbone and subsequent conversion of the chloromethyl groups into QA with aqueous trimethylamine solution. The alternative route is bromination of methylated polyaromatics and subsequent amination. These hydrocarbon polymers for tethering QA groups include polysulfone[9,10], poly(arylene ether sulfone)s[11,12], poly(arylene ether ketone)s[13,14], and poly(phenylene oxide)s[15,16]. However, QA-AEMs suffer a lot from poor alkaline stability caused by degradation of QA groups at high pH value, following two main degradation pathways, elimination and nucleophilic substitution[17]. As a potential alternative to QA cations, imidazolium with a π-conjugated structure has been suggested for enhanced alkaline stability. Therefore, a variety of imidazolium functionalized AEMs(Im-AEMs), which utilized different polymer backbones ranging from aliphatic[18] to aromatic structures[19—21] have been extensively explored. Recently, a density functional theory(DFT) calculation indicated that the degradation of imidazolium cations followed a nucleophilic addition-elimination pathway at the C2 atom position on the imidazolium ring[22]. Some experimental evidence has also confirmed that the alkaline stability of unsubstituted imidazolium is generally much too low for AAEMFC applications[23,24]. However, according to the DFT calculations, proper substitutions at the C2, C4 and C5 positions make the OH^- attack and the ring-opening step more difficult, thus improving the alkaline stability compared to unsubstituted imidazoliums. Yan's group[25,26] has investigated the alkaline stability of C2 and N3 substituted imidazolium salts. After substitution, the alkaline stability of imidazolium salts has increased significantly due to the protection of the cations by steric hindrance[25,26]. Gao *et al.*[27] investigated the alkaline stability of the poly(2,6-dimethyl-1,4-phenylene oxide) based AEMs containing methyl-substituted imidazolium cations. The ion exchange capacity(IEC) and conductivity of membranes decreased sharply after immersing in 1 mol/L KOH at 60 °C for 120 h. This observation was not consistent with the report of Yan's group[25,26]. Varcoe *et al.*[24] also suggested that the alkaline stability of benzyldimethylimidazolium cations, where acidic protons at C2 position are replaced with methyl groups was still lower than QA analogues. These observations are not

*Corresponding author. Email: huina@jlu.edu.cn

Received June 19, 2018; accepted October 12, 2018.

Supported by the National Natural Science Foundation of China(No.21474036).

consistent with the report of Yan's group[25,26], indicating that the straight introduction of substitutions at the C2 position is not enough to stabilize the imidazolium cations. The substitutions at the N3 position of imidazolium rings also play a significant role in the improving the alkaline stability of imidazolium cations. The improvement may arise from both the steric hindrance and the σ-π hyper conjugative effect between the N3 substitutions and the π-conjugated imidazole ring[25,28]. To examine this, we synthesized the polymers containing modified imidazolium cations with methyl-substituted on C2 position and alkyl-substituted on N3 position. The corresponding AEMs were also prepared and characterized in this paper.

In general, stable ionic groups and strong polymer backbones lead to good chemical stability, and higher IEC, and higher ionic conductivity. However, high IEC results in excessive water uptake and poor dimensional stability in water. It is demonstrated that constructing ionic channels in AEMs is an efficient strategy to promote ionic conductivity, even with lower IEC[13,29,30]. Designing additional hydrophobic side chains in AEMs is an effective solution as reported. Nanophase separation driven by hydrophobic side chains contributes to facilitating ionic conductivity and improving chemical stability. Li *et al.*[31] synthesized and characterized a series of comb-shaped quaternized poly(2,6-dimethyl phenylene oxide)s. Phase separation, formed by the pendent alkyl chains, enhanced the alkaline stability and ionic conductivity of AEMs, compared with membranes based on benzyltrimethyl ammonium cation. Pan *et al.*[32,33] designed a series of quaternary ammonium functionalized polysulfones with independent hydrophobic long alkyl chains. The membranes exhibited excellent ionic conductivity and dimensional stability under moderate IEC due to the ion-aggregating structure and hydrophilic/hydrophobic phase separation. It is concluded that attaching long alkyl chain onto the cationic center or onto the polymer backbone but separated from the cation is both beneficial to forming comb-shaped structures and inducing hydrophilic-hydrophobic separation. Therefore, introducing long alkyl chains at the N3 position of imidazolium cations would result in such comb-shaped hydroxide-conducting polymers.

Herein, we prepared a series of comb-shaped poly(arylene ether sulfone) AEMs containing pendent 2-methyl-3-alkylimidazolium groups(Im-PAES-C*x*). The imidazolium cations were stabilized by methyl group at the C2 position and various long alkyl chains at the N3 position. The structure and morphology of these Im-PAES-C*x* polymers were characterized by hydrogen nuclear magnetic spectra(^{1}H NMR) and small angle X-ray scattering(SAXS). The properties of the resulted AEMs with different alkyl side chains were investigated in detail, including IEC, water uptake, thermal and mechanical properties, hydroxide conductivity and alkaline stability.

2 Experimental

2.1 Materials

All reagents were purchased from commercial vendors and used without any further purification. 3,3′,5,5′-Tetramethyl-4,4′-biphenol(TMBP) was obtained from Lanzhou Aokai Chemical Company(Lanzhou, China). 4-Flourophenyl sulfone was obtained from Zhejiang Shouerfu Chemical Co., Ltd. (Hangzhou, China). Benzoyl peroxide(BPO) was obtained from Shanghai Jiachen Chemical Company(Shanghai, China). *N*-Bromosuccinimide(NBS) and 1-bromohexane were obtained from Alddin Chemistry Co., Ltd. 1-Bromodecane and 2-methylimidazole were obtained from Tianjin Guangfu Chemical Company (Tianjin, China).

2.2 Synthesis of 1-Hexyl-2-methylimidazole

1-Hexyl-2-methylimidazole was synthesized as follows (Scheme 1): a mixture of 2-methylimidazole(2.46 g, 30 mmol), 1-bromohexane(4.46 g, 27 mmol) and NaOH(1.8 g, 45 mmol) in acetonitrile(70 mL) was stirred at 60 °C for 12 h under a nitrogen atmosphere. After that, the reaction was stopped, allowed to cool to room temperature, and the solids were filtered. The solvent was removed by vacuum distillation, and the crude product was dissolved in 70 mL of CH_2Cl_2, washed with distilled water four times and dried over anhydrous $MgSO_4$. After filtration, the filtrate was concentrated *in vacuo*. ^{1}H NMR(500 MHz, DMSO-d_6), δ: 7.01(d, 1H), 6.70(d, 1H), 3.85—3.82(t, 2H), 2.26(s, 3H), 1.65—1.60(p, 2H), 1.28—1.22 (m, 6H), 0.87—0.82(m, 3H).

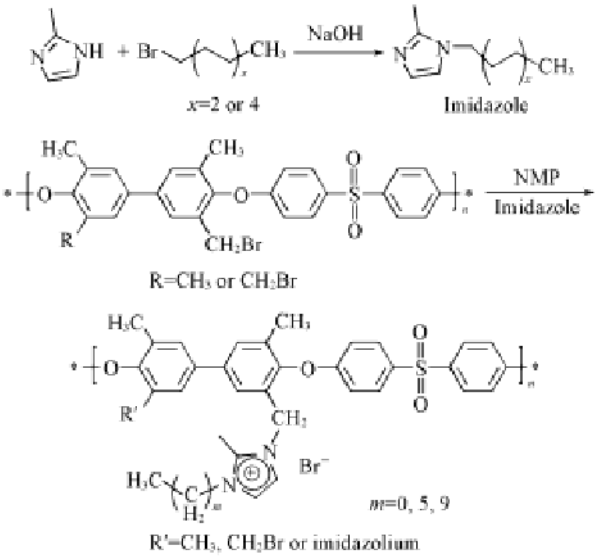

Scheme 1 Synthesis of imidazole and ImPAES-C*x* polymers

2.3 Synthesis of 1-Decyl-2-methylimidazole

1-Decyl-2-methylimidazole was synthesized using the same procedure shown in Scheme 1 with 1-bromodecane(5.97 g, 27 mmol). ^{1}H NMR(500 MHz, DMSO-d_6), δ: 7.01(d, 1H), 6.70(d, 1H), 3.84—3.82(t, 2H), 2.26(s, 3H), 1.66—1.60(p, 2H), 1.29—1.20(m, 14H), 0.88—0.85(m, 3H).

2.4 Synthesis of Brominated Poly(arylene ether sulfone)(Br-PAES)

Scheme 2 shows the preparation of Br-PAES. Firstly, a typical synthesis procedure of poly(arylene ether sulfone) (PAES) is as follows: a mixture containing 25.4 g(0.1 mol) of

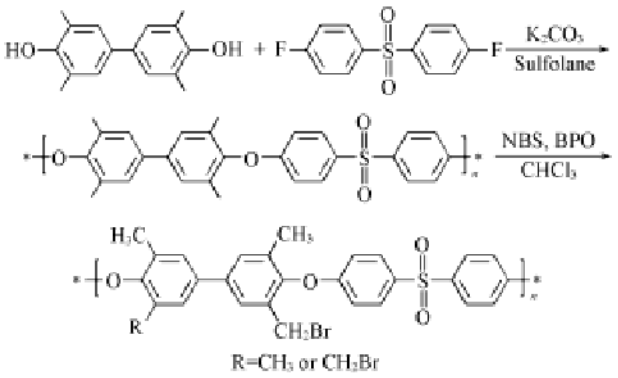

Scheme 2 Synthesis of Br-PAES

4-fluorophenyl sulfone, 24.3 g(0.1 mol) of TMBP, 15.18 g(0.11 mol) of K_2CO_3, 124 mL of sulfolane and 42 mL of toluene was added to a three-necked flask equipped with a nitrogen inlet, a mechanical stirrer and a Dean-Stark trap. The mixture was heated at 140 °C for 3 h to remove the water by azeotropic distillation with toluene. Then the reaction was heated to 200 °C and stirred for 2 h. The high viscosity mixture was coagulated into a large excess of deionized water. The precipitation was washed with deionized water several times and dried under vacuum at 80 °C for 24 h.

Secondly, the bromination of the PAES was performed according to our previous work: 15 g(33 mmol) of PAES was dissolved in 200 mL of chloroform in a three-necked flack. NBS(11.9 g, 66 mmol) and 1.60 g of BPO were added in two roughly equal portions and heated at 70 °C for 24 h. The mixture was coagulated in acetone, washed and dried.

2.5 Preparation of Imidazolium Functionalized PAES(ImPAES-C*x*)

ImPAES-C1 was prepared as follows: Br-PAES(3 g, 5 mmol) was dissolved in 30 mL of *N*-methylpyrrolidone (NMP). After that, 1,2-dimethylimidazole(1.01 g, 10.5 mmol) was added and heated at 60 °C for 12 h. The mixture was coagulated in acetone, washed and dried(Scheme 2).

ImPEAS-C6 was prepared using the same procedure above with 1-hexyl-2-methylimidazole(1.73 g, 10.5 mmol).

ImPEAS-C10 was prepared using the same procedure above with 1-decyl-2-methylimidazole(2.33 g, 10.5 mmol).

The imidazolium functionalized polymers(0.8 g) were dissolved in 10 mL of dimethylsulfoxide(DMSO). The solutions were filtered and then cast onto flat glass plates. The membranes were dried at 60 °C for 24 h to obtain flexible and tough membranes. After casting, we put the glass plate into deionized water to peel off the membranes. The membranes were immersed in 1 mol/L NaOH solution at room temperature for 48 h to obtain the OH^- form membranes. Finally, all samples were washed thoroughly and immersed in deionized water for 24 h to remove the residual NaOH.

2.6 Characterization of Membranes

^{1}H NMR spectra were measured at 500 MHz on a Bruker 510 spectrometer using deuterated dimethylsulfoxide (DMSO-d_6) or deuterochloroform($CDCl_3$) as the solvent and tetramethylsilane(TMS) as the standard. SAXS curves of wet membranes in I^- form were obtained using an Anton PaarSAXSess mc^2 instrument with a Cu *Kα* X-ray(λ=0.1542 nm). The I^- form membranes were obtained by immersing samples in 1 mol/L KI solution for 48 h and washed with deionized water for 24 h. Differential scanning calorimetry (DSC) was performed using a Mettler Toledo DSC 821e instrument heated from 50 °C to 300 °C at a heating and cooling rate of 10 °C/min under a nitrogen atmosphere to obtain the glass transition temperature(T_g). Thermogravimetry analysis(TGA) was performed on a Perkin-Elmer Pyris1 thermogravimetric analyser from 80 °C to 720 °C at a heating rate of 10 °C/min under a nitrogen atmosphere. Thermogravimetry coupled time-resolved mass spectrogram(TG/MS, Netzsch STA 449 F3 Jupiter®/QMD 403D Aëolos) was used for further study of the degradation process of Im-PAES-C*x*. Each sample was heated from 80 °C to 700 °C at a heating rate of 10 °C/min under a nitrogen atmosphere. The mechanical properties of wet samples were evaluated at room temperature on a SHIMADZU AG-I 1KN at a speed of 2 mm/min.

2.7 Water Uptake and Swelling Ratio

Membranes in the hydroxide form were immersed in deionized water at the given temperature for 24 h. After that, we took the membranes out of water, and removed the excess surface water by wiping with tissue paper. The mass and length were measured as soon as possible. After all the measurement, the membranes were vacuum-dried at 80 °C for 24 h, and then their dry mass and length were measured. The water uptake (WU) and swelling ratio(SR) were calculated by the following equations:

$$WU(\%)=[(m_w-m_d)/m_d]\times100\% \quad (1)$$

$$SR(\%)=[(L_w-L_d)/L_d]\times100\% \quad (2)$$

where, m_w and m_d are the masses of the wet and dry samples, L_w and L_d are the thicknesses of the wet and dry samples.

2.8 Ionic Conductivity

The conductivity(σ, mS/cm) was measured by a four-electrode AC impedance method from 0.1 Hz to 100 kHz, using a Princeton Applied Research Model 2273 potentiostat/galvanostat/FRA. The thickness of membranes was averaged over several measurements taken by a digital micrometer in different regions of the samples. To remove the residual ion, membranes were immersed in deionized water for 24 h before measurement. The conductivity was calculated by the following equation:

$$\sigma=l/(R\times S\times d) \quad (3)$$

where, l is the distance between the two electrodes, and R is the resistance of the membrane; S and d are the width and thickness of the membrane.

2.9 Alkaline Stability

All membrane samples in OH^- form were immersed in NaOH solution(1 mol/L) at room temperature and at 60 °C, and then we measured the hydroxide conductivity of samples with

different immersing time at room temperature.

3 Result and Discussion

3.1 Synthesis of 1-Alkyl-2-methylimidazole and Bromated Poly(arylene ether sulfone)

1-Hexyl-2-methylimidazole and 1-decyl-2-methylimidazole were synthesized by a nucleophilic substitution of 2-methylimidazolium and 1-bromohexane or 1-bromodecane, respectively. The chemical structures and purity of these 1-alkyl-2-methylimidazole compounds were confirmed by their ^{1}H NMR spectra in DMSO-d_6(as shown in Fig.1).

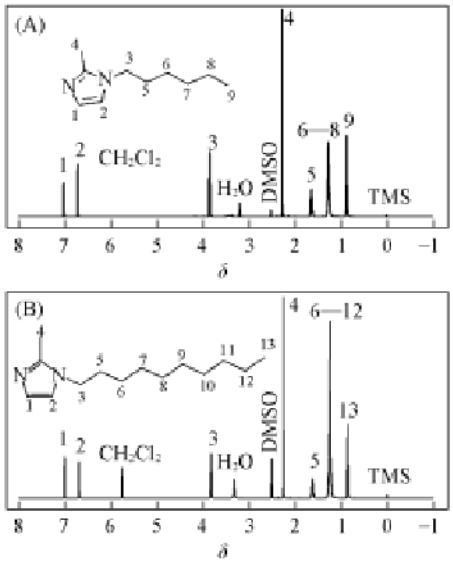

Fig.1 ^{1}H NMR spectra of 1-hexyl-2-methylimidazole(A) and 1-decyl-2-methylimidazole(B)

Br-PAES was synthesized according to our previously reported work[28]. And the ^{1}H NMR spectra of Br-PAES are shown in Fig.2. Peaks at δ 4.5 are assigned to the protons of benzyl bromide(Br-CH_2-Ar), while peaks at δ 2.2 are assigned to the protons of benzylmethyl groups(Ar-CH_3). And the degree of bromination(DB) can be calculated by integration intensity of H_1(δ 7.89) and H_2(δ 7.60). The DB of Br-PAES used in this paper is 1.75.

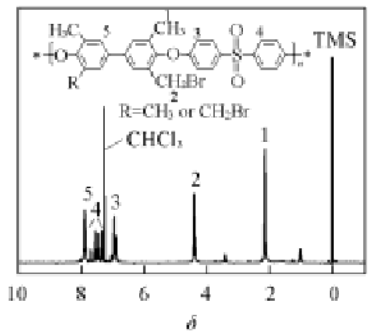

Fig.2 ^{1}H NMR spectra of Br-PAES

3.2 Characterization of Comb-shaped Imidazolium Functionalized Poly(arylene ether sulfone)

Scheme 1 shows the procedure to synthesize the comb-shaped ImPAES-C*x* polymers in Br^- form. The chemical structures were identified by ^{1}H NMR spectroscopy, and their spectra are shown in Fig.3. The appearance of peaks for alkyl chains at δ 0.8—2.1 and δ 3.9 indicates that the alkyl-substituted imidazolium cations are attached to the polymer chain successfully. The single peak at δ 5.2 is assigned to the two benzylic protons of N-CH_2-Ar. The peaks at δ 4.4 are assigned to the protons of benzyl bromide(Br-CH_2-Ar), which suggests that the conversion is not 100%. And the degree of conversion was calculated to be *ca*. 74% by the integral ratio of H6(δ 5.38) and CH_2Br(δ 4.35). The degree of imidazoulium functionalization(DF) is about 1.3, which means there are about 1.3 imidazolium cations per repeating unit of ImPAES polymers. The low degree of conversion might be attributed to the steric hindrance of imidazolium groups.

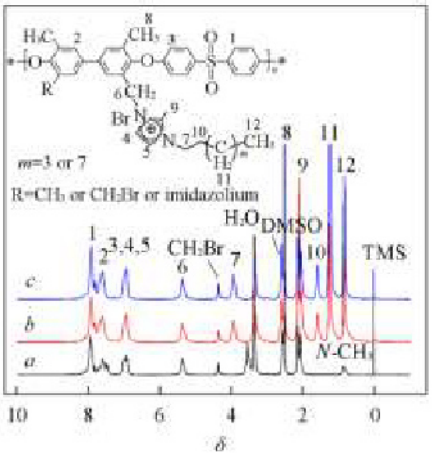

Fig.3 ^{1}H NMR spectra of ImPAES-C1(*a*), ImPAES-C6(*b*) and ImPAES-C10(*c*) in Br^- form

3.3 Morphology of ImPAES-C*x* Membranes

Quantitative information of the size of ionic cluster can be obtained from the SAXS pattern of ImPAES-C*x* membranes. The SAXS profiles of three different membranes with N3-substituted alkyl side chains(C1, C6, and C10) are shown in Fig.4. Generally, the characteristic separation length(*d*) between the ionic domains in ionomer can be derived from the values of scattering vector(*q*) corresponding to the so-called ionomer peak(d=2π/q). There is no ionomer peak observed for ImPAES-C1 membranes without long alkyl side chains attached to the imidazolium group, indicating that no characteristic phase separation is induced in such membrane. While for C6 and C10 membranes, the characteristic ionomer peaks can be observed at 3.8 and 2.4 nm^{-1}, implying that nano-phase separation with ionic domains exists in such membranes. The length scale *d* values of the corresponding periodic structure for ImPAES-C6 and ImPAES-C10 membranes are 1.65 and 2.62 nm, respectively, which roughly correspond to the length of the extended aliphatic side chains. Similar results have been reported by Li *et al*.[25] that the *d* values of quaternized poly(2,6-dimethyl phenylene oxide)s containing alkyl side chains C6 and C10 are 1.7 and 2.3 nm, respectively. The lack of the second order scattering peak indicates that the separation between hydrophobic and hydrophilic phase is only locally correlated and no long-range ordered structure forms in the

membranes. Moreover, compared with ImPAES-C6, ImPAES-C10 with the longer decylside chain shows a narrower, more obvious ionomer peak in its SAXS profile and the larger *d* value, suggesting the formation of distinct and well-separated ionic domains. The longer the alkyl side chain is introduced, the more distinct the aggregation of the ionic clusters is.

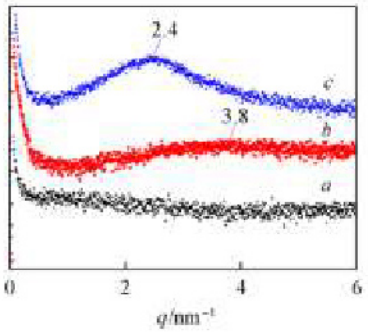

Fig.4 SAXS profiles of wet ImPAES-C1(*a*), ImPAES-C6(*b*) and ImPAES-C10(*c*) membranes in I^- form

3.4 IEC, Water Uptake Behavior and Ionic Conductivity

Table 1 shows the DF, IEC, water uptake and swelling ratio of ImPAES-C*x* membranes. The IEC values, which are calculated from their DF values, decreased from 2.09 mmol/g to 1.73 mmol/g, as the length of alkyl side chain at the N3 position of imidazolium cation increased. The decreasing trend is caused by the increasing hydrophobicity of the alkyl chain. IEC is closely related to the water uptake, swelling ratio and ionic conductivity of AEMs. Higher IEC usually results in higher water uptake and higher ionic conductivity. As shown in Table 1, the water uptake and swelling ratio of the ImPAES-C*x* membranes increase with the increasing temperature. For example, ImPAES-C1 exhibited the water uptake of 38.20% and the swelling ratio of 16.19% at 30 °C. As the temperature increased to 60 °C, the water uptake increased to 231.37% and the swelling ratio increased to 55.04%. Similar to the IEC, the water uptake and swelling ratio also decreased with the increasing alkyl chains length at given temperature. The water uptake values of ImPAES-C6 and ImPAES-C10 dramatically decreased to 90.52% and 15.66%, respectively. Compared to ImPAES-C6, these values were decreased by 61% and 93%, respectively. For the swelling ratio values of ImPAES-C6 and ImPAES-C10 with long alkyl chains, they were decreased by 50% and 68%, respectively. These results demonstrated that the hydrophobicity of alkyl chains restricted the membrane swelling efficiently, especially at high temperature. The nano-phase separation between the hydrophilic and hydrophobic domains is also believed to be responsible for the improved dimensional stability. The self-aggregated ionic domains allowed for a more continuous and cohesive hydrophobic matrix, which inhibited the water absorption and mechanical deterioration at high temperature. Above all, we can find that it is efficient to form nano-phase separation in AEMs to improve dimensional stability.

The ionic conductivity is one of the most important aspects to estimate the promising application of AEMs in alkaline fuel cells. Generally, the ionic conductivity depends on the IEC, water uptake and morphology. As shown in Fig.5, ImPAES-C6 has the highest ionic conductivity(17.2 mS/cm at 25 °C and 38.7 mS/cm at 80 °C) among these ImPAES-C*x* membranes. Although the IEC of ImPAES-C6(1.95 mmol/g) is relatively lower than that of ImPAES-C1(2.09 mmol/g), the ionic conductivity is higher than that of ImPAES-C1(12.0 mS/cm at 25 °C and 32.6 mS/cm at 80 °C). The formation of hydrophilic/ hydrophobic separation structure is advantageous to promote the hydroxide conductivity. Phase separation driven by the alkyl side chains attached to the imidazolium groups constructs ionic self-aggregated domains for effective hydroxide transportation. Unexpectedly, the ImPAES-C10 membrane (7.3 mS/cm at 25 °C and 18.8 mS/cm at 80 °C) with the longest hydrophobic alkyl chains showed the lowest hydroxide conductivity in spite of its well-defined nano-phase separated morphology. It may be caused by two reasons. First, the IEC and water uptake of ImPAES-C10 are much lower than those of ImPAES-C1 and ImPAES-C6. Second, over aggregation of ionic clusters might occur, thus resulting in lower possibility of forming interconnected of ionic channels[25]. These two factors both lead to lower hydroxide conductivity of ImPAES-C10 membrane.

Table 1 IEC, water uptake and swelling ratio of ImPAES-C*x* membranes

Sample	DF[a]	IEC[b]/ (mmol·g^{-1})	Water uptake(%)		Swelling ratio(%)	
			30 °C	60 °C	30 °C	60 °C
ImPAES-C1	1.32	2.09	38.20	231.37	16.19	55.04
ImPAES-C6	1.33	1.95	16.54	90.52	9.35	27.44
ImPAES-C10	1.32	1.73	11.96	15.66	6.93	17.82

a. DF, degree of imidazolium functionalization per repeating unit, was calculated from the ^{1}H NMR integration in Fig.3; *b*. IEC was calculated from the ^{1}H NMR integration.

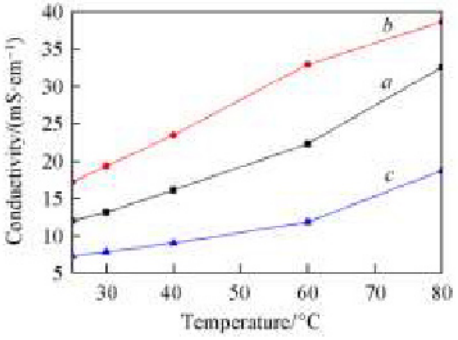

Fig.5 Hydroxide conductivity of ImPAES-C1(*a*), ImPAES-C6(*b*) and ImPAES-C10(*c*) as a function of temperature

3.5 Alkaline Stability

In addition to ionic conductivity, the alkaline stability is another crucial property that determines the long-term stability of an AEM. The degradation of AEMs in alkaline environment is generally known for *β*-H elimination and nucleophilic substitution, while the degradation of imidazolium group also undergoes the ring-open reaction, which is attributed to the attack of OH^- at C2 position. Most AEMs undergo facile removal of anion exchange groups after alkaline treatment. The hydroxide

conductivity decreased by 35%—45% after immersing in 4 mol/L NaOH for 72 h for QA functionalized PAES[34] and around 33% hydroxide conductivity reserved after hot alkaline treatment(1 mol/L KOH, 60 °C) for 48 h in the study of Dai *et al*.[35]. As demonstrated by Arges and co-workers[29], the attachment of cationic groups would also result in the polysulfone backbone hydrolysis in alkaline environment. In the work of Gao *et al*.[27], AEMs containing 2-methylimidazolium terminated long side chains suffered serious conductivity loss(declined by around 70% hydroxide conductivity after immersing in 1 mol/L KOH for 72 h).

In this work, we investigated the alkaline stability of AEMs with 2-methylimidazolium long side chain attached to the polymer main chain. All the ImPAES-C*x* membranes did not distinctly embrittle in 1 mol/L NaOH solution at room temperature and experienced less than 10% conductivity loss over the testing period, as shown in Fig.6. And after an initial period of slow degradation over the first 120 h, no significant change in conductivity was observed for these membranes. Specifically, the alkaline stability of ImPAES-C10 membrane is the best. It maintained 96% of its initial conductivity after immersing in 1 mol/L NaOH up to 170 h. Meanwhile, ImPAES-C6 and ImPAES-C1 maintained 95% and 91% of initial conductivity, respectively. The results indicated that the alkaline stability increased with the length of alkyl chains at the N3 position of imidazolium cations. Such an enhancement in alkaline stability might be explained that the long alkyl side chains induced the hydrophilic/hydrophobic separation structure, thereby separating the cationic groups and the polymer backbone. Thus, the OH^- was confined in the hydrophilic domains, and the stability of polymers was enhanced. Additionally, the steric hindrance of the alkyl chains and the σ-π hyper conjugative effect between the N-3 substitutions and the π-conjugated imidazole ring protected the 2-methylimidazolium cations from being attacked by OH^-, thus hindering the ring-open reaction of 2-methylimidazolium cations.

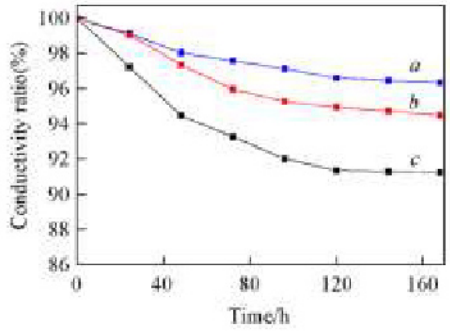

Fig.6 Time courses of hydroxide conductivity of ImPAES-C1(*a*), ImPAES-C6(*b*) and ImPAES-C10(*c*) in 1 mol/L NaOH at room temperature

3.6 Thermal Stability

The thermal stabilities of ImPAES-C*x* membranes including the glass transition temperature(T_g) and thermalgravimetry were investigated by DSC and TGA. As shown in Table 2, the thermal behavior of polymers is mainly affected by the length of pendent alkyl chains. With the length of alkyl chains at the N3 position increasing, the T_g of ImPAES-C*x* polymers decreased from 265 °C to 182 °C due to the plasticizing effect of long alkyl chains. The decomposition temperature for 5% mass loss($T_{d,5\%}$) that derived from their TGA curves also decreased from 343 °C to 284 °C with the length of alkyl chains increasing.

Table 2 Mechanical and thermal properties of ImPAES-C*x* membranes in Br^- form

Sample	T_g[a]/°C	$T_{d,5\%}$[b]/°C	Tensile strength/MPa	Elongation at break(%)
ImPAES-C1	265	343	36.4±3.6	10.6±1.0
ImPAES-C6	200	295	41.0±3.5	12.8±2.2
ImPAES-C10	182	284	38.5±2.7	11.4±1.6

a. ImPAES-C*x* in Br^- form, measured by DSC; *b*. ImPAES-C*x* in Br^- form, measured by TGA

To further investigate the decomposition process of pendent alkyl chains and polymers, TG-MS measurements were carried out. Fig.7 shows the TG-MS patterns of ImPAES-C1 and ImPAES-C10 membranes. There are three significant mass loss steps for these comb-shaped ImPAES-C*x* membranes. The initial mass loss around 100 °C was ascribed to the loss of absorbed water and solution in the sample. The second mass loss starting around 260 °C[Fig.7(A)] and 230 °C [Fig.7(B)] is due to the ring-open of imidazolium group (N—CH) and degradation of alkyl side chains(—CH_3, —$CH_2CH_2CH_3$), as shown in the TG-MS patterns. Compared with ImPAES-C1 membrane, the thermal decomposition temperature of ImPAES-C10 membrane decreased because of the introduction of alkyl side chain, as shown in Fig.7(B). And the mass loss ratio of ImPAES-C10 membrane is higher than that of ImPAES-C1 membrane, owing to the easier degradation of alkyl chain. The third mass loss starting around 340 °C is attributed to the degradation of the whole polymer backbones,

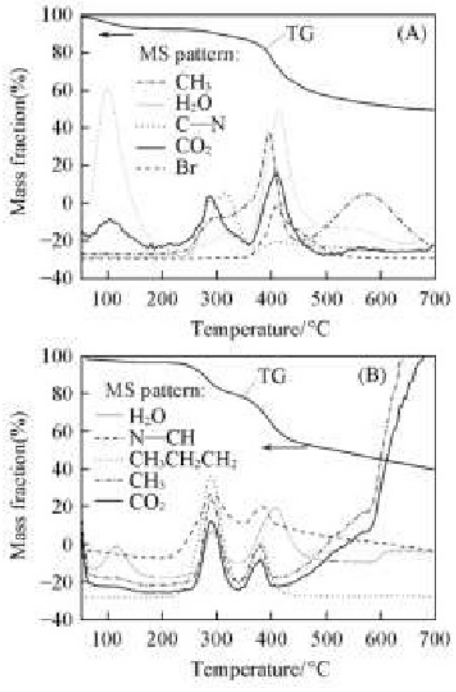

Fig.7 Thermogravimetry-MS patterns of ImPAES-C1(A) and ImPAES-C10(B) membranes

judging from the evolution of H_2O and CO_2. It can be estimated that the thermal stability of ImPAES-C6 membrane is similar to that of ImPAES-C10 membrane, owing to the similar molecular structure. Although the thermal decomposition temperature decreases with the length of alkyl chains, these comb-shaped polymers are still thermally stable within the temperature range for AEM applications.

3.7 Mechanical Properties

The mechanical properties of ImPAES-C*x* membranes were measured at room temperature and the results are listed in Table 2. ImPAES-C*x* membranes possess tensile strengths varying from 36.4 MPa to 41.0 MPa, and elongation at break ranging from 10.6% to 12.8%. Both ImPAES-C6 and ImPAES-C10 membranes with long alkyl chains exhibit better mechanical properties than ImPAES-C1 membrane. However, ImPAES-C10 membrane shows a lower tensile strength than that of ImPAES-C6 membrane. It can be explained that the long alkyl side chains entangle mutually, which strengthen the mechanical properties of both membranes. However, longer alkyl side chains in ImPAES-C10 membrane result in larger spacing between polymer backbones, which reduces the interaction force between them. These results indicate that proper long alkyl side chains endow Im-PAES membranes with excellent mechanical properties.

4 Conclusions

A series of hydroxide conductive comb-shaped poly(arylene ether sulfone)s containing pendent 2-methyl-3-alkylimidazolium group was synthesized and characterized. By homogenous functionalization, we obtained membranes with good solubility in polar aprotic solvents, excellent dimensional stability and mechanical properties, together with enhanced alkaline stability. The ImPAES-C6 membrane showed a combination of improved hydroxide conductivity, dimensional stability and alkaline stability, which is attributed to the formation of nano-phase separation caused by proper length of alkyl side chains.

References

[1] Varcoe J. R., Slade R. C. T., *Fuel Cells*, **2005**, 5(2), 187

[2] Varcoe J. R., Atanassov P., Dekel D. R., Herring A. M., Hickner M. A., Kohl P. A., Kucernak A. R., Mustain W. E., Nijmeijer K., Scott K., Xu T. W., Zhuang L., *Energ. Environ. Sci.*, **2014**, *7*(10), 3135

[3] Spendelow J. S., Wieckowski A., *Phys. Chem. Chem. Phys.*, **2007**, *9*(21), 2654

[4] Sakamoto T., Matsumura D., Asazawa K., Martinez U., Serov A., Artyushkova K., Atanassov P., Tamura K., Nishihata Y., Tanaka H., *Electrochim. Acta*, **2015**, *163*, 116

[5] Wang Y. J., Qiao J., Baker R., Zhang J., *Chem. Soc. Rev.*, **2013**, *42*(13), 5768

[6] Xu H., Fang J., Guo M., Lu X., Wei X., Tu S., *J. Membr. Sci.,* **2010**, *354*(1/2), 206

[7] Dong X., Hou S., Mao H., Zheng J., Zhang S., *J. Membr. Sci.*, **2016**, *518*, 31

[8] Hu B., Miao L., Bai Y., Lu C., *Polym. Chem.*, **2017**, *8*(30), 4403

[9] Wang G., Weng Y., Chu D., Chen R., Xie D., *J. Membr. Sci.*, **2009**, *332*(1/2), 63

[10] Weiber E. A., Jannasch P., *J. Membr. Sci.*, **2016**, *520*, 425

[11] Zhao Z., Wang J., Li S., Zhang S., *J. Power Sources*, **2011**, *196*(10), 4445

[12] Gong X., Yan X., Li T., Wu X., Chen W., Huang S., Wu Y., Zhen D., He G., *J. Membr. Sci.*, **2017**, *523*, 216

[13] Chen D., Hickner M. A., *Macromolecules*, **2013**, *46*(23), 9270

[14] Xu S., Zhang G., Zhang Y., Zhao C., Zhang L., Li M., Wang J., Zhang N., Na H., *J. Mater. Chem.*, **2012**, *22*(26), 13295

[15] Xu T. W., Liu Z. M., Yang W. H., *J. Membr. Sci.*, **2005**, *249*(1/2), 183

[16] Yang J., Liu C., Hao Y., He X., He R., *Electrochim. Acta*, **2016**, *207*, 112

[17] Couture G., Alaaeddine A., Boschet F., Ameduri B., *Prog. Polym. Sci.*, **2011**, *36*(11), 1521

[18] Qiu B., Lin B., Si Z., Qiu L., Chu F., Zhao J., Yan F., *J. Power Sources*, **2012**, *217*, 329

[19] Zhang F., Zhang H., Qu C., *J. Mater. Chem.*, **2011**, *21*(34), 12744

[20] Rao A. H. N., Nam S., Kim T. H., *Int. J. Hydrogen Energ.*, **2014**, *39*(11), 5919

[21] Pan Y., Zhang Q., Yan X., Liu J., Xu X., Wang T., Hamouti I. E., Ruan X., Hao C., He G., *J. Membr. Sci.*, **2018**, *552*, 286

[22] Long H., Pivovar B., *J. Phys. Chem. C*, **2014**, *118*(19), 9880

[23] Wang W., Wang S., Xie X., Lv Y., Ramani V. K., *J. Membr. Sci.*, **2014**, *462*, 112

[24] Deavin O. I., Murphy S., Ong A. L., Poynton S. D., Zeng R., Herman H.,Varcoe J. R., *Energ. Environ. Sci.*, **2012**, *5*(9), 8584

[25] Lin B., Dong H., Li Y., Si Z., Gu F., Yan F., *Chem. Mater.*, **2013**, *25*(9), 1858

[26] Gu F., Dong H., Li Y., Si Z., Yan F., *Macromolecules*, **2014**, *47*(1), 208

[27] Gao L., He G., Pan Y., Zhao B., Xu X., Liu Y., Deng R., Yan X., *J. Membr. Sci.*, **2016**, *518*, 159

[28] Yang C., Wang S., Ma W., Jiang L., Sun G., *J. Mater. Chem. A*, **2015**, *3*(16), 8559

[29] Arges C. G., Ramani V., *Proc. Natl. Acad. Sci. USA*, **2013**, *110*(7), 2490

[30] Ran J., Wu L., Xu T., *Polym. Chem.*, **2013**, *4*(17), 4612

[31] Li N. W., Leng Y. J., Hickner M. A., Wang C. Y., *J. Am. Chem. Soc.*, **2013**, *135*(27), 10124

[32] Pan J., Chen C., Zhuang L., Lu J. T., *Accounts Chem. Res.*, **2012**, 45(3), 473

[33] Pan J., Chen C., Li Y., Wang L., Tan L. S., Li G. W., Tang X., Xiao L., Lu J. T., Zhuang L., *Energ. Environ. Sci.*, **2014**, *7*(1), 354

[34] Hu Z., Tang W., Ning D., Zhang X., Bi H., Chen S., *Fuel Cells*, **2016**, *16*(5), 557

[35] Dai J., He G., Ruan X., Zheng W., Pan Y., Yan X., *Int. J. Hydrogen Energ.*, **2016**, *41*(25), 10923